Experimental Study of Ductile Fracture of Tubes Under Combined Tension/Torsion

by

Joseph M. Johnson

Submitted to the Department of Mechanical Engineering
in Partial Fulfillment of the Requirements for the Degree of

Bachelor of Science

at the

Massachusetts Institute of Technology

June 2007

Signature of Author .....
Department of Mechanical Engineering
May 11, 2007

Certified by .....
Tomasz Wierzbicki
Professor of Applied Mechanics
Thesis Supervisor

Accepted by .....
John H. Lienhard V
Professor of Mechanical Engineering
Chairman, Undergraduate Thesis Committee

Experimental Study of Ductile Fracture of Tubes
Under Combined Tension/Torsion

by

Joseph M. Johnson

Submitted to the Department of Mechanical Engineering
on May 11, 2007 in partial fulfillment of the
requirements for the Degree of Bachelor of Science in
Mechanical Engineering

ABSTRACT

This experiment sought to compare the results of an experimental torsion test on a specimen of 1045 steel with a torsion simulation in the ABAQUS FEA software program. A simulation of a tension test on a round bar of 1045 steel was first executed to determine the correct stress-strain curve for 1045 steel. A torsion specimen was designed based on the constraints of the testing machine, and the torsion test was carried out. A model of the specimen was constructed in ABAQUS using the results of the tension simulation, and a torsion test was simulated. The simulation accurately predicted the shape of the experimental torque vs. twist curve, but the simulated values were 7% higher than the experimental values in the plastic region. The specimen fractured at a rotation of 43° with a plastic strain of 1.013. This was 2.4 times higher than in the tension simulation, where the specimen failed at a strain of 0.427.

Thesis Supervisor: Tomasz Wierzbicki

Title: Professor of Applied Mechanics

Table of Contents

Abstract **2**

Table of Contents **3**

1 Introduction **4**

2 Material Property Calibration

2.1 Tensile Test 4

2.2 Tensile Test Simulation 6

2.3 Mesh-Size Effect 12

3 Torsion Specimen Design and Testing

3.1 Design of Specimen 13

3.2 Torsion Testing 16

4 Simulation of Torsion Test **18**

5 Conclusions **20**

References **22**

1. Introduction

In this experiment, the results of a torsion test on an Instron testing machine will be compared with a finite element simulation in ABAQUS. A tension test on a round bar of 1045 steel was first performed to determine the correct stress-strain curve for the material. Various mesh sizes for the model were also compared, and the results of these tests were used in the torsion simulation. Finally, a torsion specimen of 1045 steel was designed for a torsion test, and the test was carried out. The results will be used to examine the fracture strains for the tension and torsion tests and the ability of the finite element simulations to predict the behavior of the tests.

2. Material Property Calibration

2.1 Tensile Test

The correct stress-strain curve for 1045 steel first needed to be calibrated. To accomplish this, a tension test was performed on a round bar of 1045 steel, and the test was also simulated in ABAQUS. The specimen used in the tensile test is shown in Figure 1.

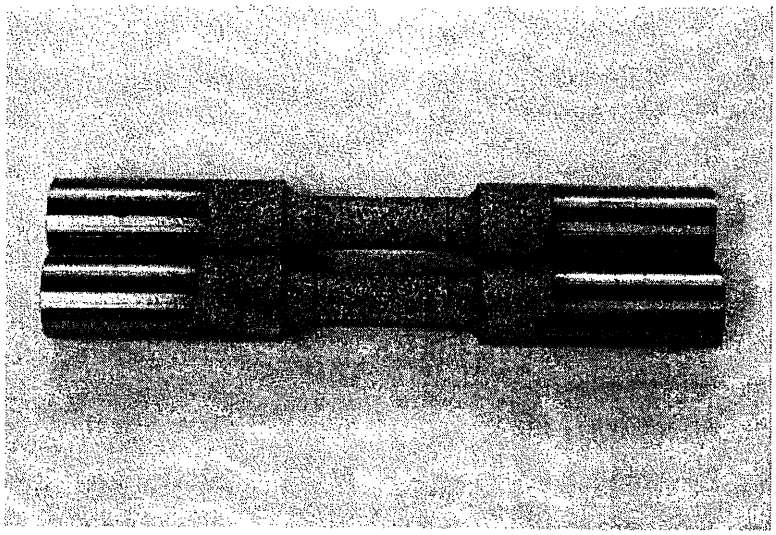

Figure 1: Example of round specimen used in the tensile test.

The initial gauge length of the round bar was 20.56 mm, and the initial diameter was 9 mm. The force on the specimen and change in length of the specimen were recorded during the test. The relationship between these values is shown in Figure 2.

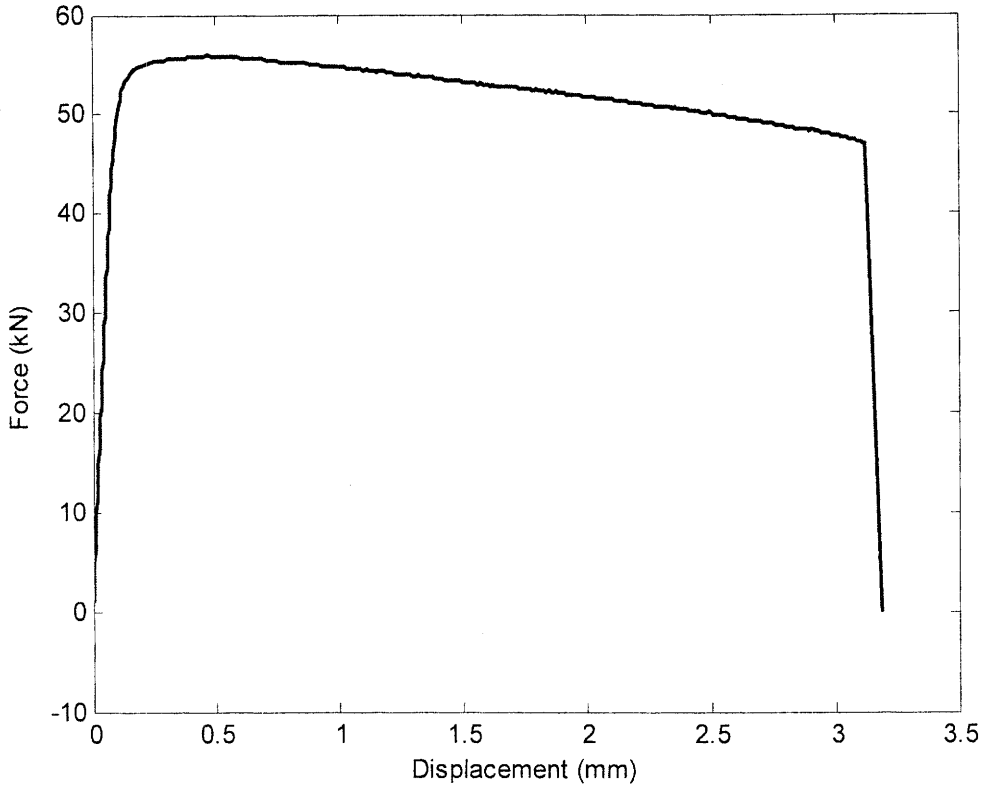

Figure 2: Force vs. displacement from tensile test.

Figure 3 shows the fractured specimen after the test. It is evident that some necking occurred in the specimen before fracture.

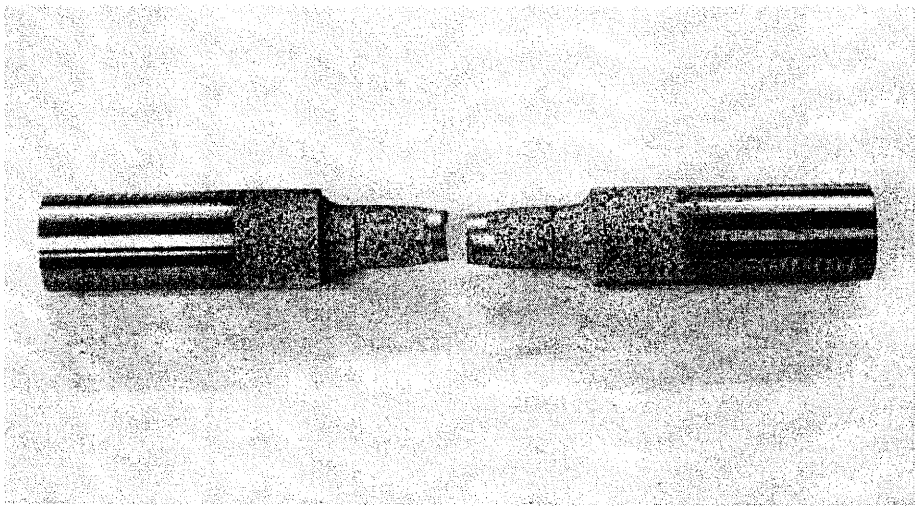

Figure 3: Specimen after undergoing tensile test.

2.2 Tensile Test Simulation

This same tensile test was also simulated in ABAQUS. A snapshot of the model is shown in Figure 4.

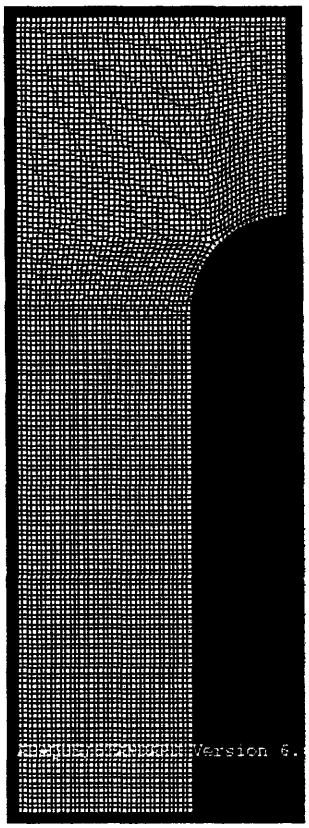

Figure 4: Cross-section of tensile specimen model in ABAQUS. Symmetry about the y- and z-axes was used to create the full model of the specimen.

The Young's modulus of 1045 steel was estimated to be 220 GPa, and the Poisson's ratio was estimated to be 0.3. The mass density used for the simulation was 7.8 $\times$ 10^3 kg/m^3. The force on the specimen and change in length of the specimen were recorded in ABAQUS during the simulation, and the result is shown in Figure 5.

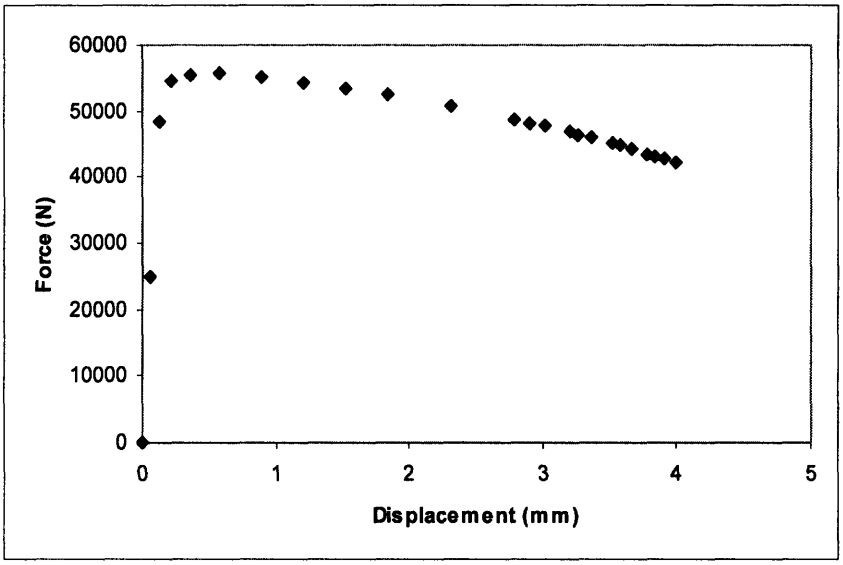

Figure 5: Force-displacement values from ABAQUS simulation using the power hardening rule, Equation (7).

These values were used to calculate the engineering strain E and engineering stress S using Equations (1) and (2).

$$E = \frac{d}{L_0} \tag{1}$$

$$S = \frac{F}{A_0} \tag{2}$$

where d is the displacement, L_0 is the initial length of the specimen, F is the force, and A_0 is the initial area of the specimen. Inserting the force and displacement values from the simulation into these equations results in the engineering stress-strain curve shown in Figure 6.

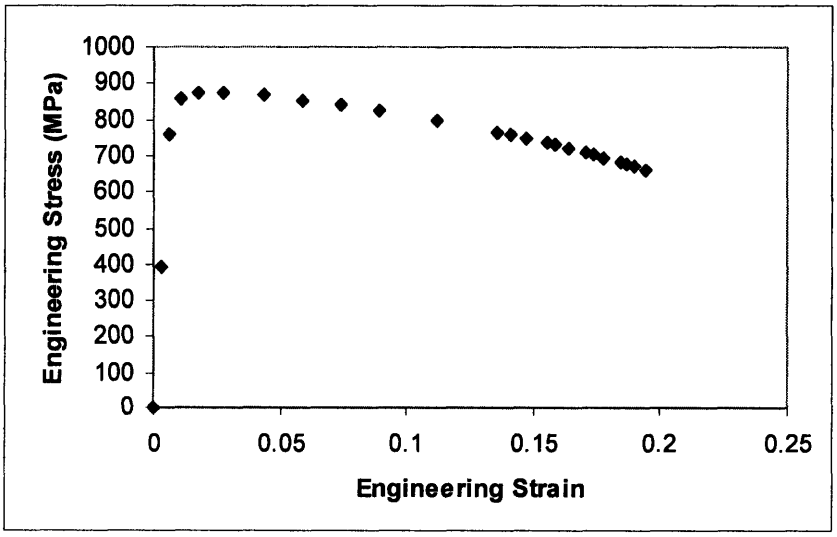

Figure 6: Engineering stress-strain curve from tensile test.

Equations (3) and (4) were used to convert the engineering stress and strain to true stress σ and true strain ε.

$$\sigma = S(1+E) \tag{3}$$

$$\varepsilon = \ln(1+E) \tag{4}$$

The true stress-strain curve is shown in Figure 7.

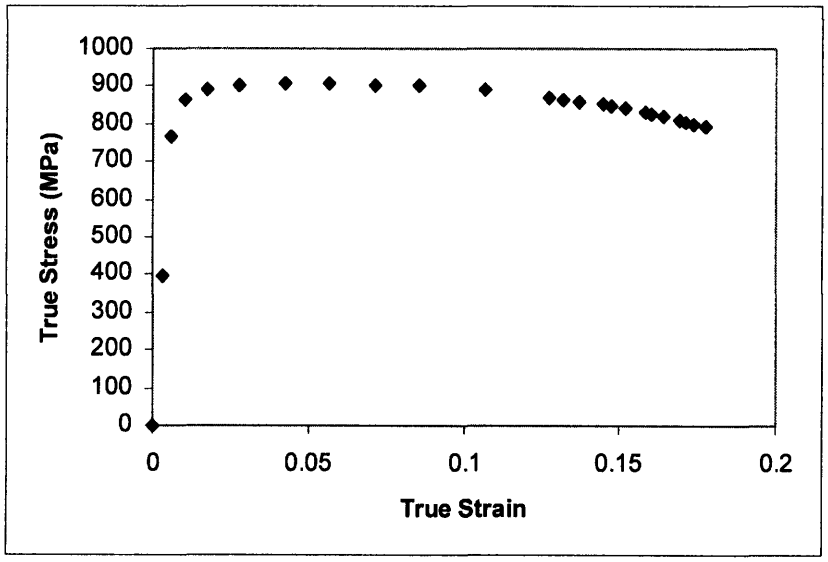

Figure 7: True stress-strain curve from test and Equations (3) and (4).

Figure 8 shows the stress concentrations in the model immediately before fracture.

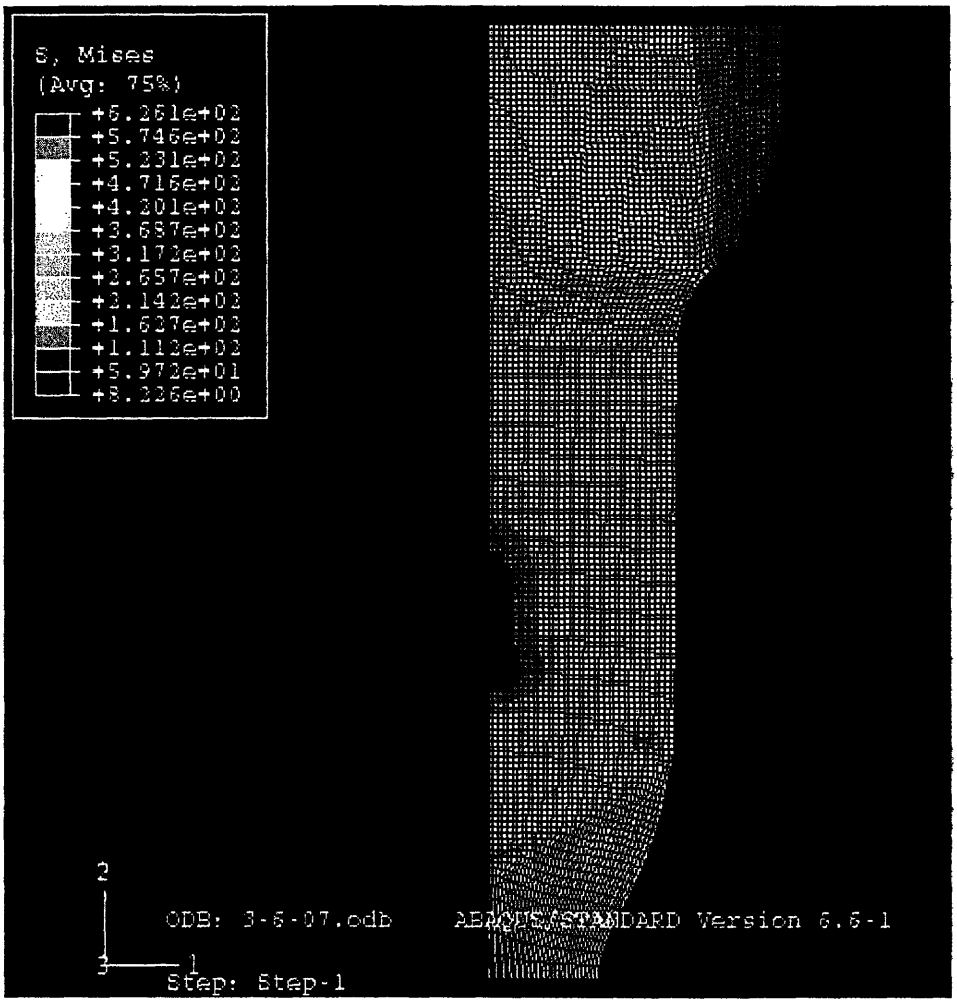

Figure 8: Stress concentrations in ABAQUS model just before fracture.

Both the simulation and experimental test show that necking occurs during a tensile test on 1045 steel. The relationships in Equations (1) – (4) are only valid before necking occurs in the specimen. Figure 9 shows where necking begins on the stress-strain curve.

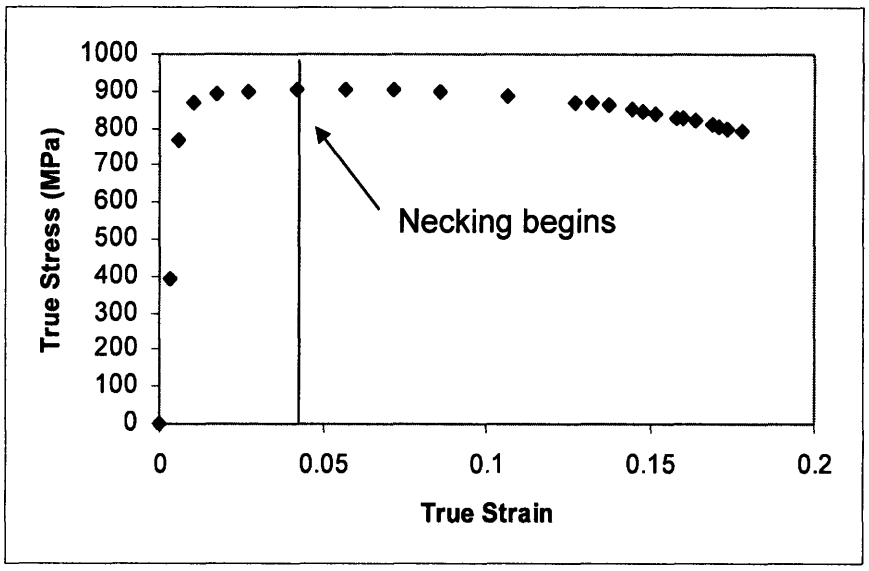

Figure 9: True stress-strain curve showing the onset of necking.

The points to the left of the vertical line are the only points that may be used. The remainder of the stress-strain curve must be estimated based on an exponential function fit to the "pre-necking" portion of the curve. This function is in the form

$$\bar{\sigma} = \sigma_0 + A\left(\bar{\varepsilon}^p\right)^n \tag{5}$$

where $\bar{\sigma}$ is the stress, σ_0 is the initial stress, $\bar{\varepsilon}^p$ is the plastic strain, and A and n are constants. σ_0 in this case is 766 MPa. Taking the natural log of both sides of Equation (5) results in

$$\ln\left(\bar{\sigma} - \sigma_0\right) = \ln A + n\ln\left(\bar{\varepsilon}^p\right). \tag{6}$$

Equation (6) is a linear equation in the form

$$Y = nX + B, \tag{7}$$

where Y is $\ln\left(\bar{\sigma} - \sigma_0\right)$, X is $\ln\left(\bar{\varepsilon}^p\right)$, and B is $\ln A$. The constants n and A can now be determined from a simple linear fit to the data. The stress and plastic strain values before necking were inserted into Equation (7), and the resulting curve is shown in Figure 10.

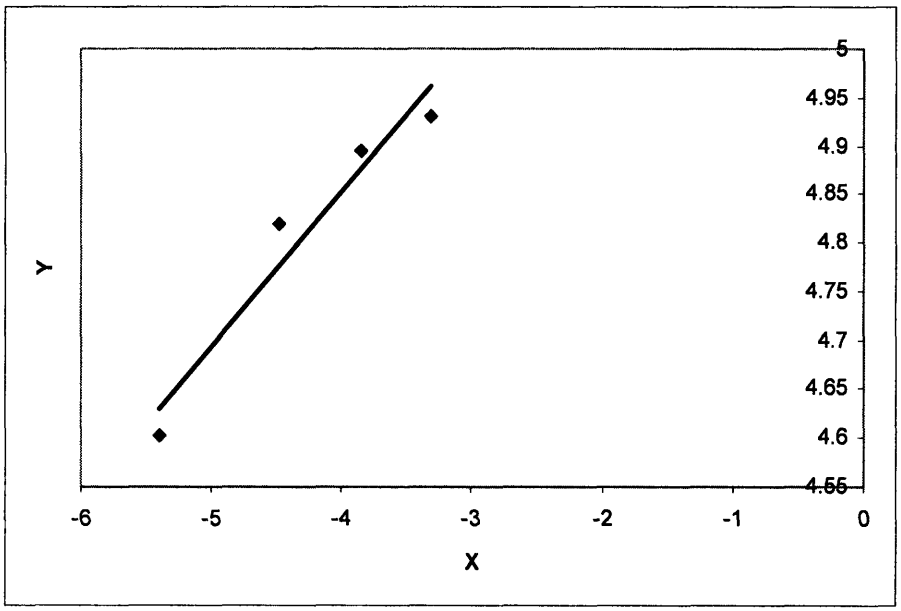

Figure 10: Natural log of stress and strain values with a line fit to the data.

The slope of the best-fit line is n and the y-intercept is ln A. For the best-fit line in Figure 10, n is 0.16 and A is 242. The function fit to the stress-strain curve is thus

$$\bar{\sigma} = 766 + 242\left(\bar{\varepsilon}^{p}\right)^{0.16}. \tag{7}$$

The strain values after necking can now be estimated using this function. The full strain-stress curve is shown in Figure 11.

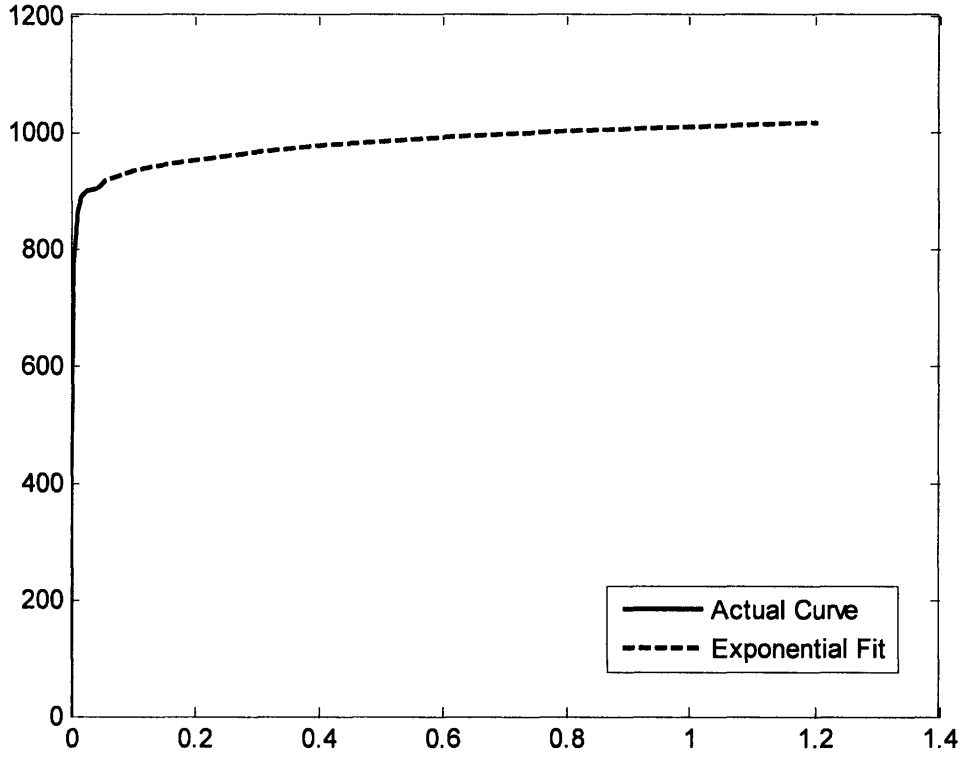

Figure 11: Strain-stress curve with the addition of the exponential fit.

2.3 Mesh-Size Effect

The finite element simulation will behave differently based on the size of the mesh that is used to mesh the part. The force-displacement curve will converge as the mesh size becomes smaller. The mesh size must to be small enough to have small errors in the force and displacement values, but large enough so that the software can run the simulation within a reasonable amount of time. The simulation was run using multiple different mesh sizes, and the resulting force-displacement curves are compared in Figure 12.

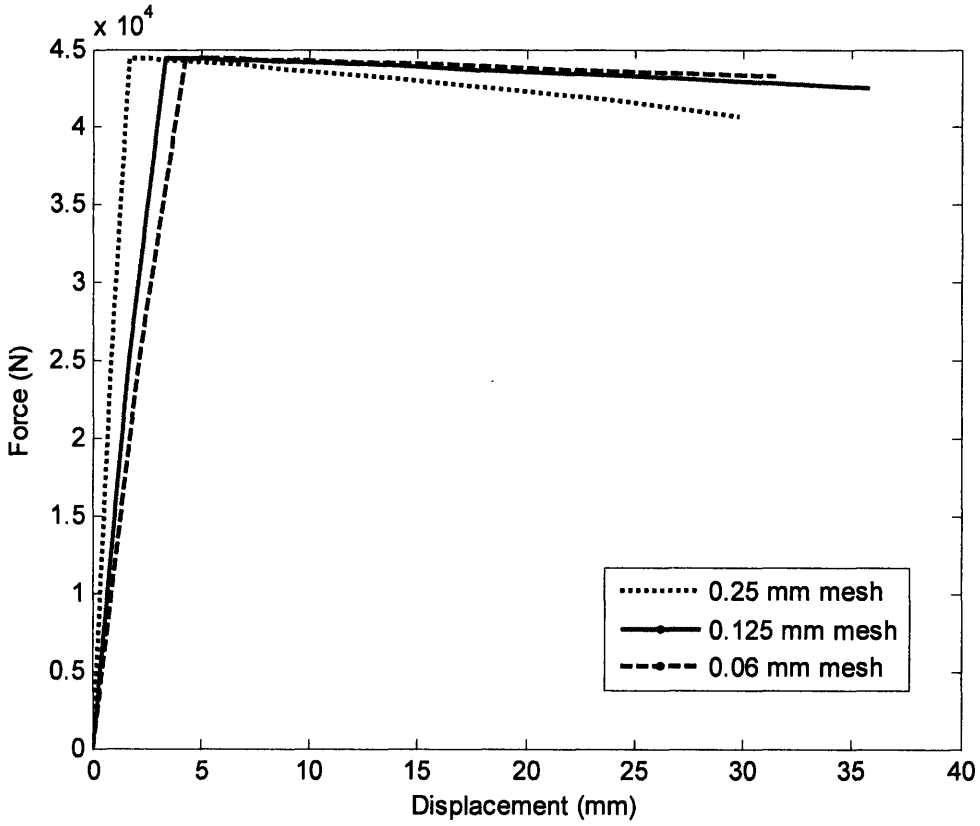

Figure 12: Force-displacement curves for various mesh sizes.

The maximum error between the 0.25 mm mesh and the 0.125 mm mesh was 3.8%. The error between the 0.125 mm mesh and anything smaller was less than 1%, so 0.125 mm was chosen as the mesh size for the simulation.

3. Torsion Specimen Design and Testing

3.1 Design of Specimen

A hollow specimen of 1045 steel was designed to undergo a torsion test. The specimen is shown in Figure 13.

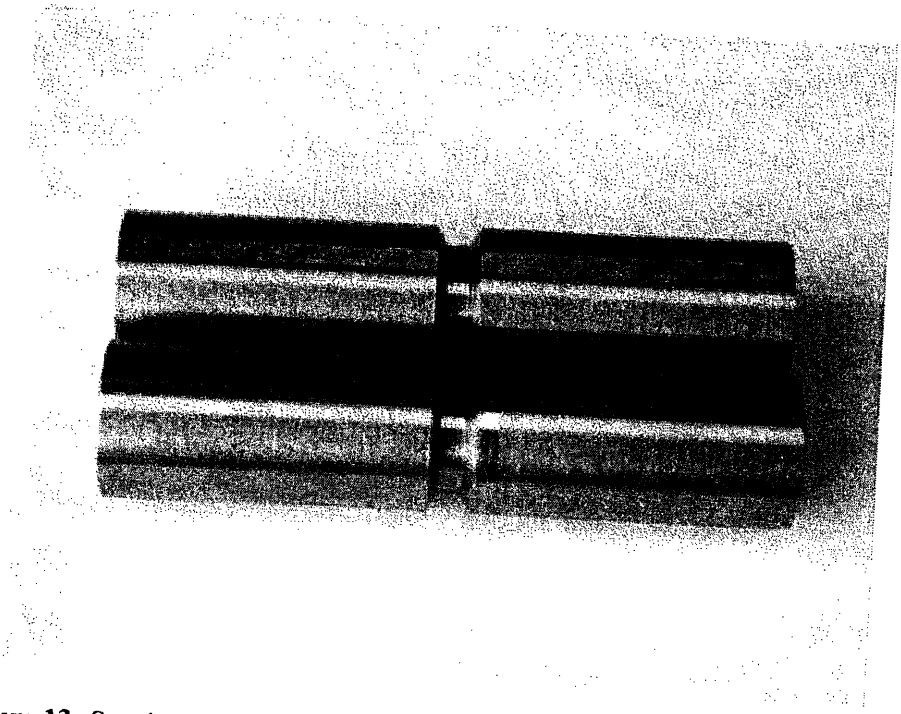

Figure 13: Specimen designed to undergo a torsion test.

The torsion test was performed on an Instron 50 Kip/20 Kip-in/10,000 psi high stiffness, precision aligned, tension/torsion/internal-pressure machine. The machine is shown in Figure 14.

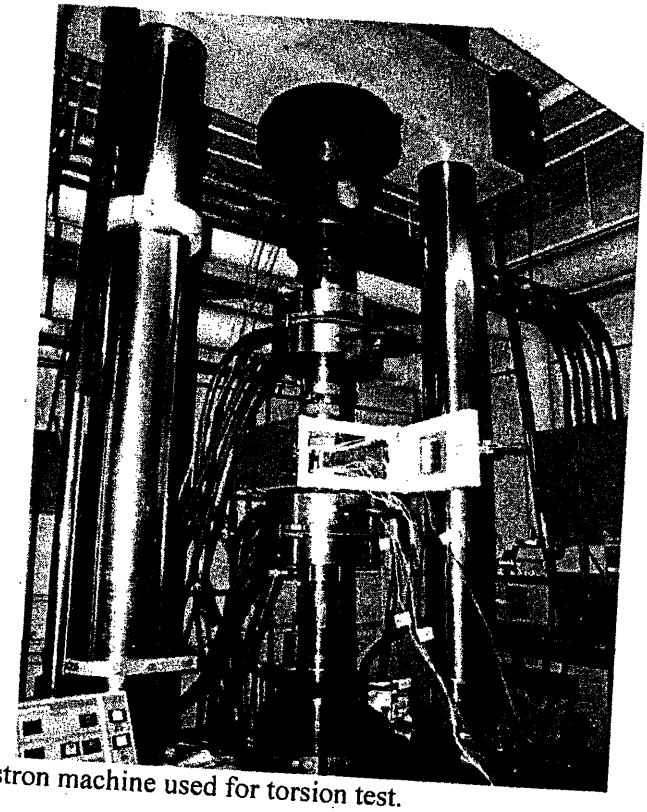

Figure 14: Instron machine used for torsion test.

The specimen was designed to yield between 250-300 N-m, at a value that would not come too close to the upper limits of the machine. The yield torque T_y can be expressed as

$$T_y = \frac{\sigma_y}{\sqrt{3}} \frac{J}{R_o} \tag{8}$$

$$J = \frac{\pi\left(R_o^4 - R_i^4\right)}{2} \tag{9}$$

where σ_y is the yield stress, J is the polar moment of inertia, and R_o and R_i are the outer and inner radii of the specimen, respectively. The outer and inner radii were chosen to be 19 mm and 16 mm, respectively. This results in a yield torque of 271 N-m. The full dimensions of the specimen are shown in Figure 15.

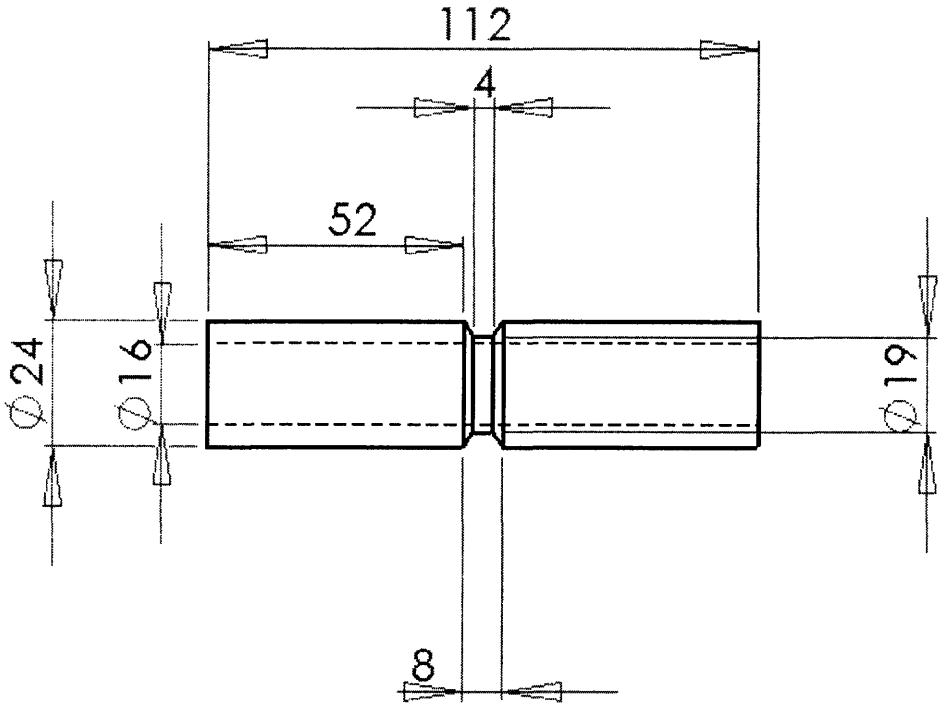

Figure 15: Dimensions of torsion specimen. All dimensions are in millimeters.

3.2 Torsion Testing

After being machined, the designed specimen underwent a torsion test on the Instron machine. Data acquisition during the test was accomplished with PCs equipped with high-speed analog-to-digital converters. The torque and twist data that was captured during the test is shown in Figure 16.

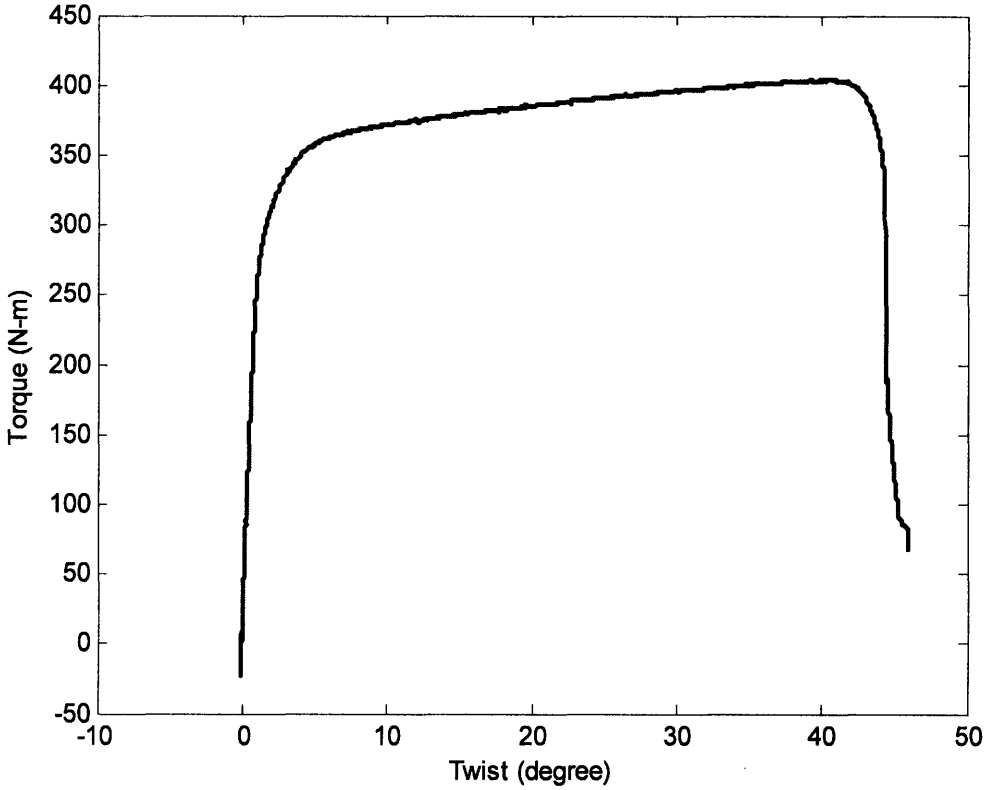

Figure 16: Experimental torque vs. twist data.

Figure 17 shows two specimens after torsion tests. One specimen was allowed to fracture and one was taken out of the machine just before fracture.

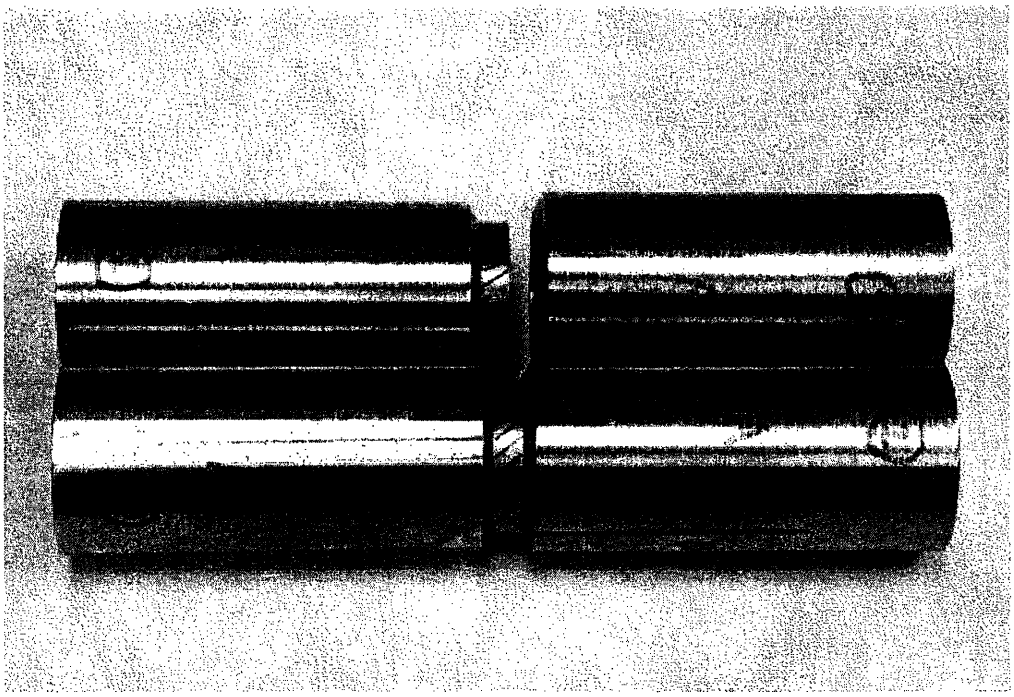

Figure 17: Two torsional specimens after undergoing torsion tests.

The lines on the center of the specimen were horizontal before the test, so it is evident that the two sides of the specimen rotated about 45° with respect to each other. Another view of the fractured specimen is shown in Figure 18.

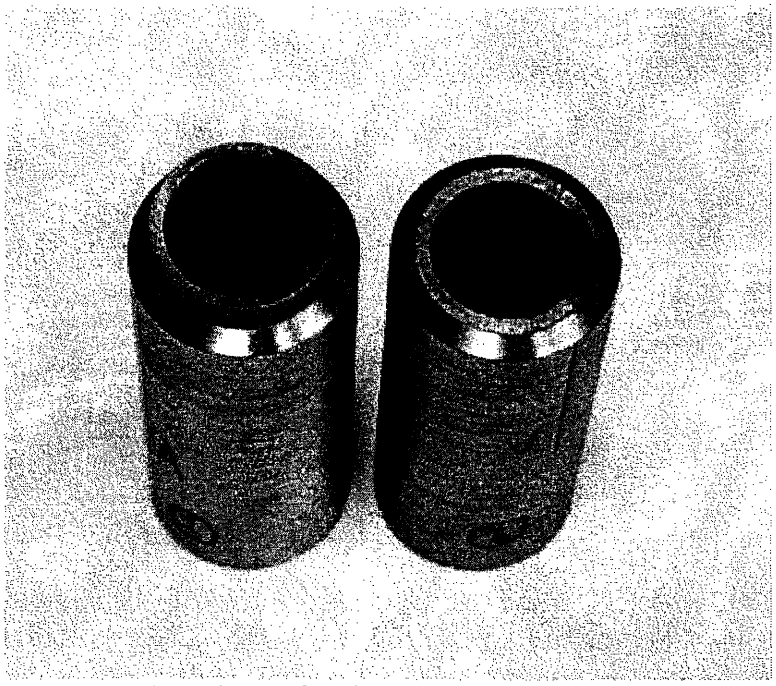

Figure 18: Fractured specimen after the torsion test.

4. Simulation of Torsion Test

A model of the torsion specimen was constructed in ABAQUS. A snapshot of this model is shown in Figure 19.

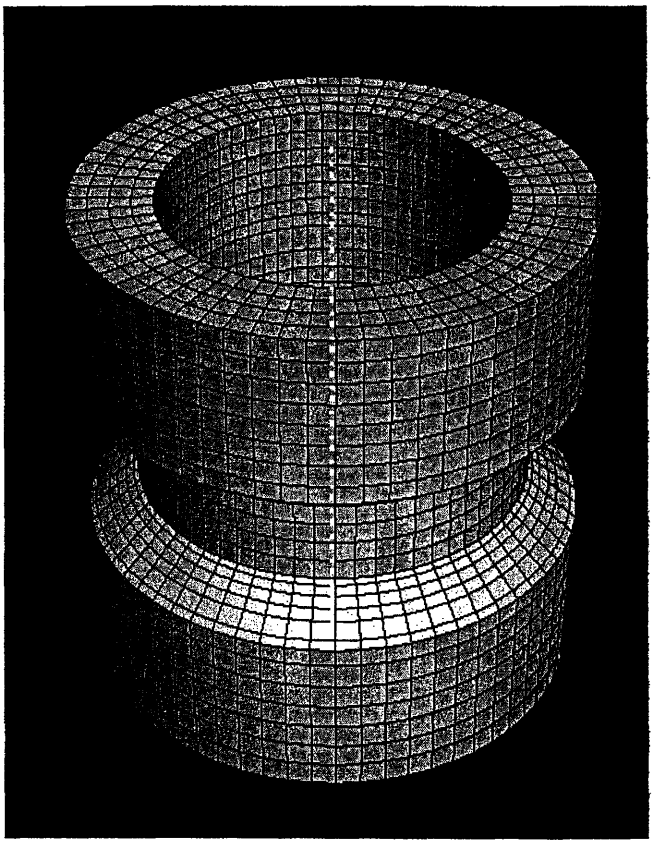

Figure 19: Model of torsion specimen in ABAQUS.

Values of 220 GPa for the Young's modulus, 0.3 for the Poisson's ratio, and 7.8 × 10^3 kg/m^3 for the mass density were again used in this simulation. The values from the stress-strain curve in Figure 11 were used for the plasticity values. The torsion test was simulated in ABAQUS, and the result is shown in Figure 20.

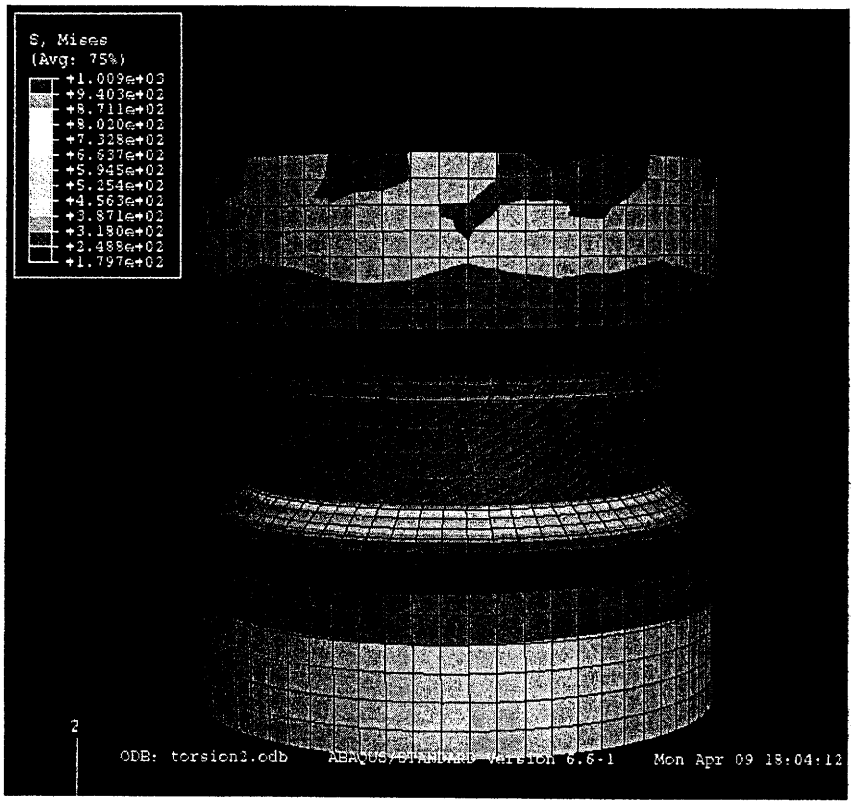

Figure 20: Deformed shape after the simulation was run showing the amount of stress in the specimen.

The torque-twist curve from the simulation is shown in Figure 21.

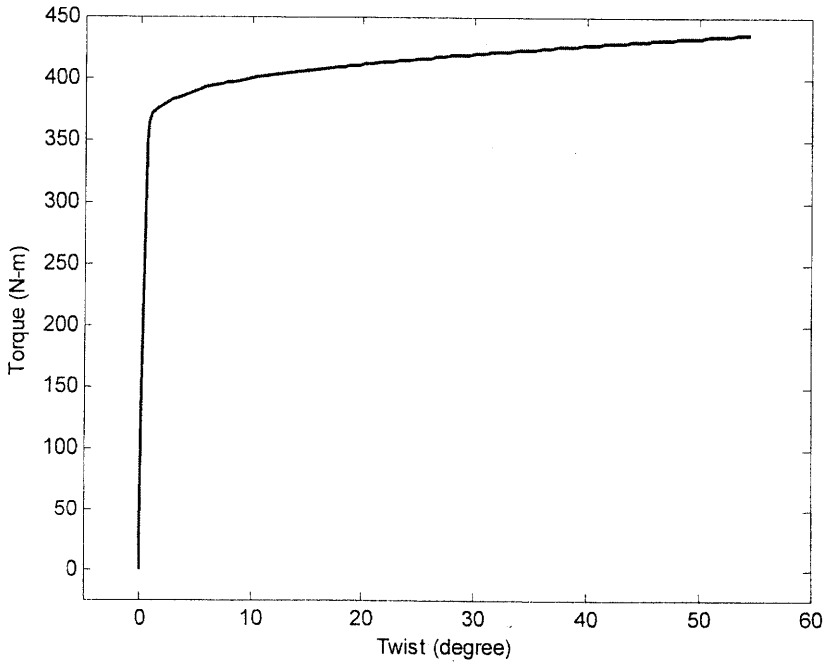

Figure 21: Torque-twist curve from ABAQUS simulation.

5. Conclusions

The force-displacement curve from the tensile test is compared with the F-d curve from the tension simulation in Figure 22.

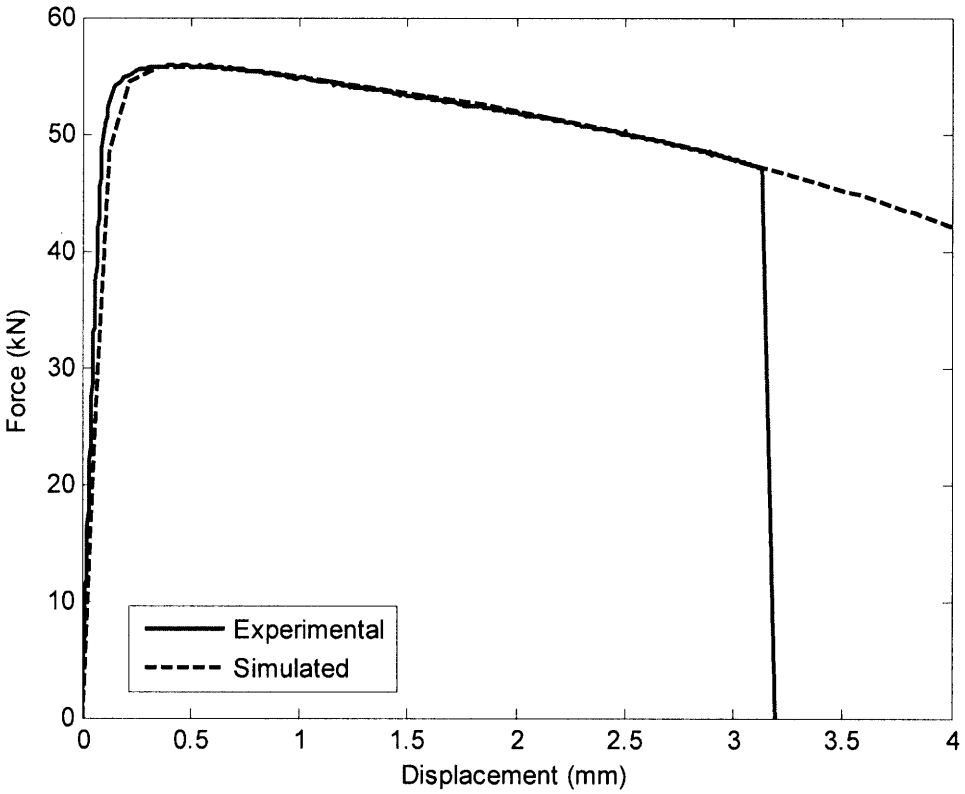

Figure 22: Experimental and simulated force-displacement curves.

The torque vs. twist curve from the torsion test is plotted with the simulated torque vs. twist curve in Figure 23.

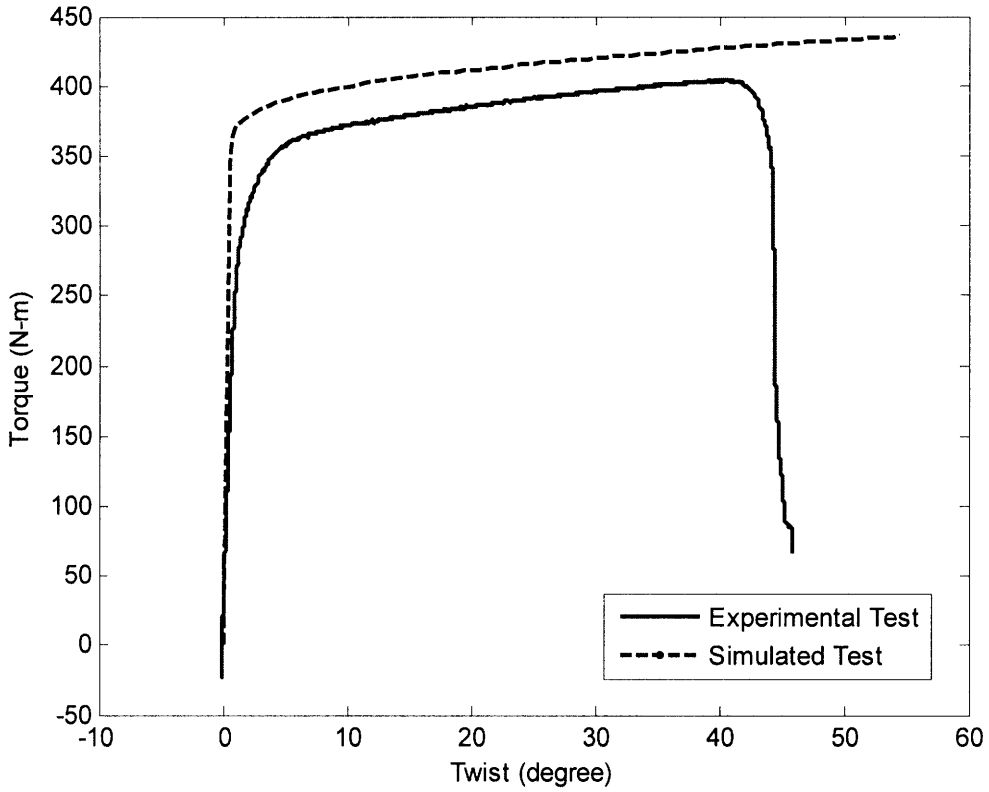

Figure 23: Comparison of simulated and experimental torque-twist curves.

ABAQUS does a much better job of simulating the tension test than the torsion test. In both cases, the greatest discrepancy comes in the transition from the elastic region to the plastic region.

Although the transition to from the elastic to the plastic region is not quite gradual enough, the simulation accurately predicted the shape of the torque-twist curve. The simulated and experimental torque values in the elastic region were almost exactly similar, but in the plastic region, the simulated values were approximately 7% higher than the experimental.

The specimen fractured at a 43° rotation during the experiment. In the simulation, the maximum plastic strain on the specimen at 43° of rotation was 1.013. This means that the specimen fractured at a strain of 101% during the torsion experiment.

In the tension simulation, the diameter of the specimen at fracture was 7.27 mm. The original diameter was 9 mm. The equivalent fracture strain can be expressed as

$$\bar{\varepsilon}_f = 2\ln\left(\frac{d_o}{d_f}\right). \tag{9}$$

In this case $\bar{\varepsilon}_f = 0.427$, or 42.7%. Thus the strain needed to cause the specimen to fracture in torsion was 2.4 times higher than that in tension.

References

1. Y. Bao and T. Wierzbicki. "Determination of Stress-strain Relations Up to Fracture for Ductile Materials." Unpublished, Impact & Crashworthiness Lab, MIT.